

# S-BAND HIGH DUTY PHOTO-INJECTION SYSTEM\*

X.J. Wang<sup>†</sup>, M. Babzien, X.Y. Chang, D. Lynch, S. Pjerov, M. Woodle and Z. Wu  
 NSLS, BNL, Upton, NY 11973, USA

## Abstract

The critical issue for the high-duty operation of the photocathode RF gun injector is the heat load for both RF gun and laser system. We have developed a complete design of a high-duty S-band photocathode RF gun injector based on the BNL GUN IV for the LCLS X-ray SASE FEL project. The complete injector consists of a photocathode RF gun, photocathode and laser system. The thermal stress of the S-band photocathode RF gun was analyzed for heat load up to 3 kW. The Mg cathode with quantum efficiency of 0.2% will be used. The laser system will be an all solid state laser consisting of a diode pumped Yb:glass oscillator and a single stage regenerative Yb:glass amplifier. This laser system is capable of operating at 120 Hz with 1 mJ energy/pulse. Simulations show that, this system is capable of producing 100 A peak current with normalized rms emittance less than 1 mm-mrad.

## 1 INTRODUCTION

With successful experimental demonstration of saturation and characterization of Self Amplified Spontaneous Emission (SASE) Free Electron Laser (FEL) [1-3], a detailed engineering design of a X-ray FEL now is possible[4]. We report the present status of the photoinjector design study for the proposed Linac Coherent Light Source (LCLS) to be built at the SLAC. This report is a further refinement of our earlier report [5].

After a brief review of the basic parameters of the photoinjector system, we will present the thermal analysis and thermal stress analysis for the RF power heat loads 1.5 kW, 2.5 kW and 3kW. We then present a preliminary design of an all solid-state laser system capable of driving the RF gun at 120 Hz. One of the most important decision of the latest design is to exclusive usage of Mg cathode for LCLS application. This is mainly due to experimentally demonstrated higher quantum efficient and smaller thermal emittance of the Mg cathode.

## 2 HIGH-DUTY PHOTO-INJECTOR SYSTEM

Figure 1 illustrates the basic components of the photoinjector system. It consists of a 1.6 cell photocathode RF gun, a single emittance compensation solenoid magnet and a small bucking coil, laser and electron beam diagnostics stations. Laser and laser beam delivery system make the rest of the system.

For the high-duty photoinjector operation, thermal loading and stress for both RF gun cavity and laser system are main concern. Stability and reliability of the photoinjector system is primarily determined by the laser system and its synchronization to the RF system. We have considered both normal and oblique laser beam delivery systems for the RF gun. To facility the laser beam diagnostics and simplified the operation, oblique incident is preferable. The complexity caused by such optical setup can be addressed with simple wave front correction optics and cylindrical lens. This is now being used routinely at the ATF for more than 5 years.

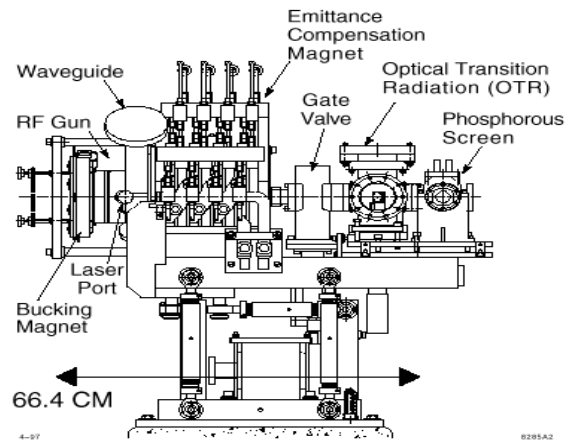


Figure 1: Photo-injector system.

Table 1: 120 Hz RF gun

RF gun rep. Rate (Hz)	120
Field on the cathode (Mv/m)	100 - 120
Cathode material	Mg
Vacuum inside the gun	$< 5 \times 10^{-10}$ Torr with RF on
Operating Temperature (°C)	15

### 2.1 High-duty Photocathode RF gun

Table 1 summarizes all basic parameters for the high-duty S-band RF gun. To reduce the heat load and improve the reliability of the Mg cathode operation, we lowered the peak acceleration field from 140 MV/m to 120 MV/m. All our simulations show that, for a normal operating field of 100 MV/m, it is capable of delivering the performance required for the LCLS. Instead of operating at 45 °C like SLAC linac, lowering the operating temperature to 15 °C

\* Supported by US DOE contract DE-AC02-98CH10886

<sup>†</sup>xwang@bnl.gov

will be implemented. This has two advantages, one is to reduce the RF gun heat load by about 10%, and it will also improve RF gun vacuum.

To further improve the RF gun vacuum, we are now proposing to coat the laser port tubes in the half-cell with NEG film.

### 2.2 Mg cathode

Based on the operating experience of Mg cathode at the ATF in the last three years, and new understanding of thermal emittance and latest experimental data [6], Mg cathode will be employed for high-duty S-band RF gun.

The present ATF Mg cathode was welded on the Copper cathode back plate using friction welding at about 250 °C. Experimental data shows that, photo-emission from Mg cathode in a strong RF field is Schottky dominated, surface photoemission process. Since such process primarily occurs within the layer of 50 Å thickness, good vacuum is critical ( $>5 \times 10^{-10}$  Torr), it will keep the life time of the cathode on the order of month before cathode cleaning.

Mg cathode has several advantages over other cathode material. ATF Mg cathode routinely has operating quantum efficiency (QE) of 0.2%, good QE will significantly simplify the laser system. Furthermore, since Mg is bulk material, it can be cleaned in-situ using vacuum based laser cathode cleaning technique to restore the QE and keep the QE variation less than 10%. We developed vacuum based laser cathode cleaning technique to avoid possible laser damage to the cathode and effective removal of nano-meter thick oxidized Mg. Using a laser spot about 0.2 mm radius, laser energy is increased while monitoring the vacuum. A factor of two increase in vacuum (initial vacuum at low minus 10) will insure the success while avoid cathode damage. We have 100% success rate with vacuum based laser cathode cleaning technique at the ATF in the last three years.

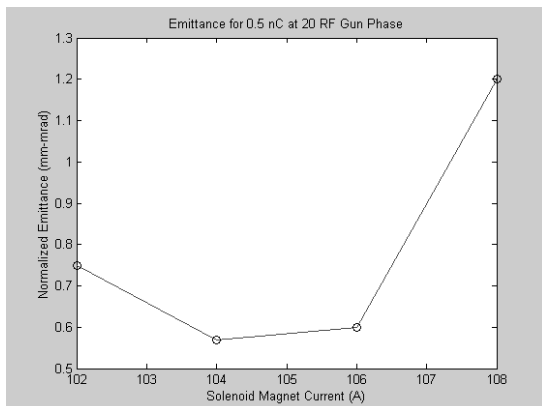


Figure 2: emittance as a function solenoid magnet field.

One of the most important reasons for using Mg cathode is that, it produces smaller thermal emittance comparing to Copper cathode [6]. As pointed out in the previous section, photoemission in the Mg cathode is dominated by the surface emission. And the mis-match between the

photon energy and Mg work function does not lead to thermal emittance. Instead, conservation of momentum will lead to photoelectrons move in the direction perpendicular to the surface. Our experimental data show that, thermal emittance for the Mg cathode is less than 0.4 mm-mrad for a 1 mm radius. Figure 2 shows measured emittance for a 0.5 nC charge at a 20 deg. RF gun phase is about  $0.6 \pm 0.2$  mm-mrad [7].

### 3 THERMAL ANALYSIS

Thermal finite element analysis (FEA) soft ware ALGOR was used to investigate the thermal distribution for RF gun heat load 1.5 kW, 2.0 kW and 3.0 kW. Superfish was first used to generate power dissipation distribution along the RF gun surface. This distribution was input into a spread sheet program to prepare for thermal analysis. Figure 3 shows the temperature distribution for the 3 kW case. Table 2 summarizes the temperature difference for all three cases.

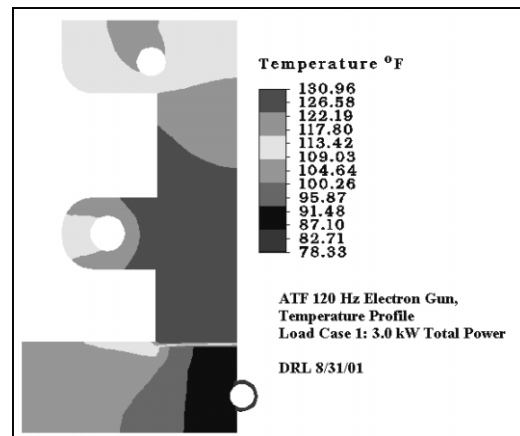


Figure 3: temperature distribution for 3 kW heat load.

Table 2: Summary of temperature distribution

Case	Max. Temp.	Max. Temp. Difference
1.5 kW	102.50 F	12.09 F
2.0 kW	112.05 F	16.21 F
3.0 kW	130.96 F	24.24 F

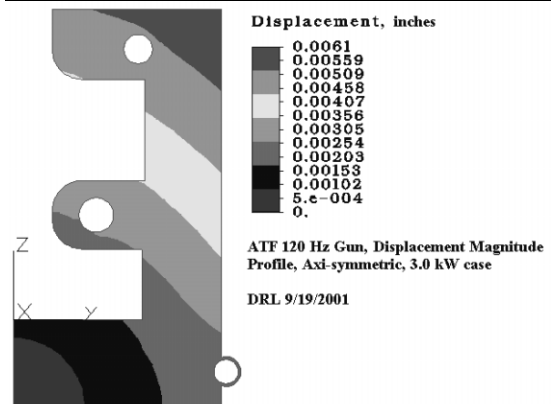


Figure 4: thermal displacement for 3 kW heat load.

Figure 4 shows the thermal stress displacement for the 3 kW RF heat load. The large frequency shift (a few MHz) due to the thermal displacement must be addressed. Since LCLS will be operating in a single-pulse mode, we can shorten the RF pulse flat part to about 500 ns without compromise RF stability. The main source of heating then comes from build-up and decay of the RF field in the gun cavity. Using the similar technique for thermionic RF gun, we can over couple the cavity to reduce build-up time from 800 ns to 500 ns with reasonable reflected power. By combing operating at the lower temperature and over couple the RF gun, we can keep the heat load of the RF gun to about 1 kW. The thermal distortion now is well within the tuner range. Our previous generation gun has demonstrated this performance [8].

### 4 LASER SYSTEM

Table 3 summarizes the laser system required to drive this RF gun. The 30 uJ UV laser is about a factor of three to six required to produce 0.5 to 1 nC charge from the Mg cathode. This build-in safety margin will serve several purposes. It is mainly to prepare for further laser pulse shaping near the cathode if situation warrants. The laser system we are now proposed is Yb:glass based, all diode pumped solid state laser with build-in longitudinal and transverse laser pulse shaping. Figure 5 is the schematic

of the laser system. The passive mode-lock oscillator is synchronized with the RF system. It then followed by a longitudinal laser pulse shaper – Acoustic-Optic Programmable Dispersive Filter (AOPDF). The femto-second laser pulse is stretched to nano-second using a fiber stretcher. A single stage regenerative amplifier will capable of producing 1 mJ output at the 120 Hz. The phase plate was used in the amplifier to generate super-gaussian mode to reduce the hot spot. Fiber coupled diode pump laser will improve the efficiency and reduce the crystal heat load. The amplified laser is compressed using grating compressor for its flexibility. We will first compress the laser to a relative shorter pulse (<5 ps) to improve the nonlinear conversion efficiency. This pulse should be stretched to about 10 ps later. The transverse laser profile can be controlled by a deformable mirror. Electron beam can be used to optimize the laser pulse shape.

Table 3: 120 Hz laser system

Rep. Rate (Hz)	120	
Energy on cathode (UV, uJ)	30 (Mg)	
Pulse length (ps, FWHM)	5 to 15	
Laser spot (radius, mm)	0.5 – 1.5	
Laser energy stability (%)	1.5 (rms)	6 (p-p)
Timing jitter (ps)	0.1	0.5 (p-p)
Point stability (%)	0.25	1

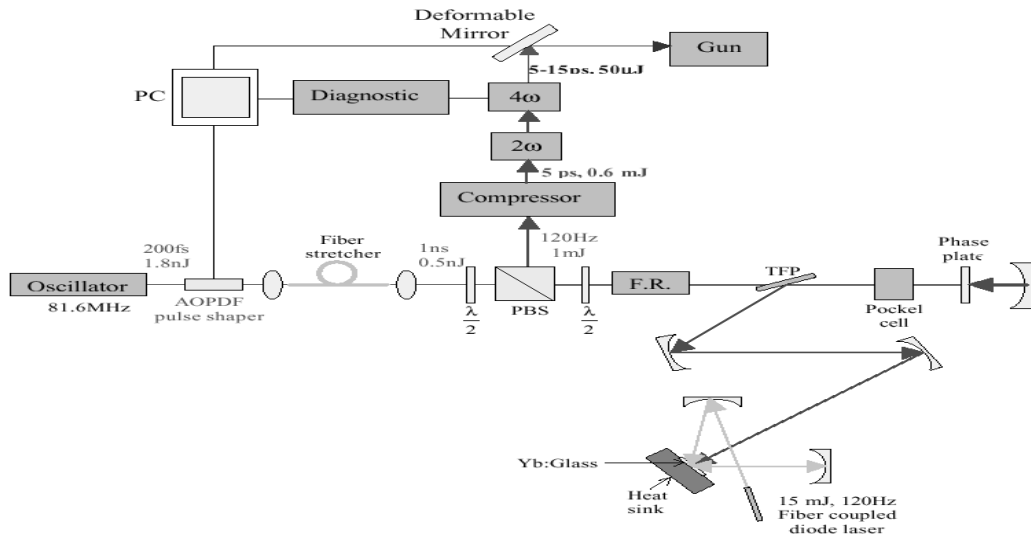


Figure 5: schematic of the proposed laser system.

### 5 ACKNOWLEDGEMENT

Authors would like to thank our SLAC colleague for many helpful discussions. The support from NSLS and BNL director office are greatly appreciated.

### 6 REFERENCES

[1] S. Milton *et al*, *Science*, 292 (2001) 2037-2041.

[2] V. Ayvazyan *et al*, *Phys. Rev. Lett.*, 88, 104802 (2002).  
 [3] A. Tremaine *et al*, *Phy. Rev. Lett.* 88, 204801 (2002).  
 [4] LCLS Conceptual Design Report, April 2002.  
 [5] X.J. Wang *et al*, PAC'01, p.2233 (2001).  
 [6] X.J. Wang *et al*, "Mg Cathode and Thermal Emittance", LINAC'02, August, 2002.  
 [7] X.J. Wang *et al*, "High-brightness Photoelectron Beam from Mg Cathode", FEL'02, September, 2002.  
 [8] F. Sakai *et al*, BNL – 65003 (1997).